Title

Tide-salinity patterns reveal seawater-freshwater mixing behavior at a river mouth and tidal creeks in a tropical mangrove estuary

Authors

Atekwana, Eliot A
Ramatlapeng, Goabaone J
Ali, Hendratta N
et al.

Publication Date

2022-12-01

DOI

10.1016/j.jafrearsci.2022.104684

Journal of African Earth Sciences 196 (2022) 104684

Contents lists available at ScienceDirect

Journal of African Earth Sciences

journal homepage: www.elsevier.com/locate/jafrearsci

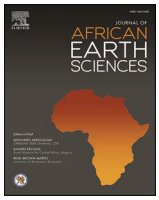

Tide-salinity patterns reveal seawater-freshwater mixing behavior at a river mouth and tidal creeks in a tropical mangrove estuary

Eliot A. Atekwana [a,*], Goabaone J. Ramatlapeng [a], Hendratta N. Ali [b], Isaac K. Njilah [c], Gustave R.N. Ndondo [d]

[a] Department of Earth and Planetary Sciences, University of California, Davis, CA, 95616, USA
[b] Department of Geosciences, Fort Hays State University, Hays, KS, 67601, USA
[c] Department of Earth Sciences, The University of Yaounde I, Yaounde, Cameroon
[d] Department of Geosciences, The University of Douala, Douala, Cameroon

ARTICLE INFO

Keywords:
Seawater-freshwater mixing
Tidal creeks
Mangrove estuary
Wouri Estuary
Cameroon
Time-series observations

ABSTRACT

Tide and salinity data collected at minute intervals over multiple semidiurnal tides were used to investigate the source of water (e.g., seawater, river, groundwater and rain) and their relative timing in mixing at the mouth of a river, a tidal creek at mid-estuary and a tidal creek at the shoreline at the head of a tropical mangrove estuary. Our objectives were to document the temporal changes in tide induced water level changes and salinity at each location and to use the relationship between salinity and water level to elucidate the sources of water and the timing of different sources of water in the hydrologic mixing processes. The data trends in tide vs. salinity (T-S) plots for the river mouth revealed mixing with seawater during rising tides and freshwater diluted seawater (brackish) drainage from the mangrove forest during ebb tides. In the mangrove creek at mid-estuary, the data trends in the T-S plots for rising tides initially showed constant salinity, followed by sharp rises in salinity to peak tide caused by seawater intrusion. The salinity decreased precipitously at the start of tidal ebbing due to influx of freshwater (rain) diluted brackish water from the mangrove forest. The data trends in the T-S plots for the tidal creek at the shoreline located at the estuary head showed constant salinity which decreased only near peak rising tide because of river dilution. During tidal ebbing, the salinity further decreased from groundwater influx before increasing to background salinity, which stayed constant to low tide. Establishing T-S patterns for multiple locations in mangrove estuaries over sub-tidal to tidal scales define the expected salinity variations in seawater-freshwater mixing which can be used to (1) establish baseline hydrologic and salinity (hydrochemical) conditions for temporal and spatial assessments and (2) serve to guide short to long-term sampling regimes for scientific studies and estuarine ecosystem management.

1. Introduction

The exchange of water, mass and energy is important in controlling the hydrologic and hydrochemical (salinity) regimes of tropical mangrove estuaries (Mitra, 2020a; Mazda et al., 1990; Rivera-Monroy et al., 2007; Smith et al., 2012; Twilley, 1985). The shifts in the hydrochemical behavior at different locations within a mangrove estuary are primarily driven by variations in water properties that are induced by interaction between waters from multiple sources such as seawater, river water, groundwater and rain (Akamatsu and Ikeda, 2016; Mazda, 2013; Mazda et al., 1990). Flow dynamics plays an important role in modulating the mixing of seawater and freshwater (rainfall, groundwater and river water) in the open water portions of estuaries and the tidal creeks connecting the open water to the mangrove forests (e.g., Alongi, and Brinkman, 2011; Mazda and Wolanski, 2009, Wolanski et al., 2000). Additionally, the hydrologic exchange of water between the open water and mangrove forests facilitates the mobilization of chemical species between sources and sinks, which controls the salinity status, biogeochemical processes, and the overall functioning of the estuarine ecosystems (Koné and Borges, 2008; Krumme et al., 2012; Mitra, 2020b; Smith et al., 2012). To adequately elucidate controls on hydrochemical patterns of water across mangrove estuaries, there is a need to understand hydrologic interactions between seawater-freshwater and the resultant mixing behaviors at multiple

* Corresponding author.
E-mail address: eatekwana@ucdavis.edu (E.A. Atekwana).

https://doi.org/10.1016/j.jafrearsci.2022.104684
Received 15 January 2022; Received in revised form 17 June 2022; Accepted 4 August 2022
Available online 10 August 2022
1464-343X/

locations in mangrove estuaries. Few studies have been conducted and even fewer models developed to assess the hydrologic and salinity behavior during tidal flooding and ebbing at different locations in mangrove estuaries (Robson et al., 2008; Webb, 1981).

On a spatial basis, estuaries with extensive mangrove forests are heterogeneous due to their diverse ecosystems with variations in mangrove species, age, structure, distribution, and their varying connections to the open water via tidal creeks (Augustinus, 1995; Lugo and Snedaker, 1974). On a temporal basis, the tidal and riverine forces that control hydrologic mixing in the open water and mangrove forest vary over short timescales associated with storms and tides or over longer seasonal to annual timescales associated with river discharge and sea level change (Jones et al., 2020). The complex ecological patterns observed in mangrove estuaries is the result of temporal environmental variability caused by changing physical and chemical properties of water (e.g., Guerreiro et al., 2021; Loveridge et al., 2021). In addition, the temporal and spatial environmental variability cause physiological and behavioral responses in organisms that affect their spatial location in time, and ultimately drive changes in population and community dynamics (Dubuc et al., 2021). Thus, to gain further insights in the hydrogeochemical processes in mangrove estuaries in support of scientific studies and estuarine management, it is necessary to characterize how the salinity and hydrogeochemistry are influenced by hydrologic mixing of different source waters at multiple locations in a mangrove estuary.

To determine the proportion of seawater and freshwater and their interaction at a given location in a mangrove estuary, we can use the relationship between hydrology and salinity. This is doable because salinity is conservative (Fry, 2002; Lewis, 1980; Loder and Reichard, 1981). Therefore, the relationship between hydrologic variations and salinity can be used to qualitatively or quantitatively determine the proportions of seawater and freshwater, and therefore elucidate the process that dominates the seawater-freshwater mixing dynamics at different locations in estuaries. The relative proportion of seawater and/or freshwater in any representative volume of estuarine water can be determined from the salinity measured by micro-electrodes (salinometer; Brown and Hamon, 1961), if one assumes linear mixing between seawater and freshwater endmembers. In addition, a salinometer can record high frequency salinity data (minute interval or less) over multiple tidal cycles (e.g., at sub-tidal scales and longer) which is tedious to do manually. A proxy for the tidal volume of seawater and freshwater can be determined from water level changes measured electronically by pressure transducers. The unknown tide volume at multiple locations in the mangrove estuary can then be normalized using water level, and the normalized water level and its associated salinity can be used to evaluate seawater-freshwater mixing.

In this study, we collected a 96 h time series data of water level and salinity at minute intervals in a tropical mangrove estuary and assessed tidal variations and salinity changes at the mouth of a river, in a tidal creek in the mangrove forest at mid-estuary and a tidal creek along the shoreline bordered by a mangrove forest at the estuary head. Our objectives were to document the temporal changes in tide induced water level changes and salinity at each location and to use the relationship between salinity and water level to elucidate the sources of water and the timing of different sources of water in the hydrologic mixing processes. Our results show that the tide-salinity behavior at the river mouth, the tidal creek at mid-estuary and the tidal creek at the shoreline near the estuary head are characteristically unique and capture salinity variations in hydrologic mixing at sub-tidal scale. Tide-salinity patterns therefore offer a robust approach for scientists and estuarine resource managers to document the salinity and consequently biogeochemical status simultaneously at multiple locations, which can be used to gain greater understanding of the role of temporal and spatial hydrologic mixing in mangrove estuaries.

2. Study area

The Wouri Estuary (3°42′0.00″N to 4°11′0.00″N and 9°14′0.00″E to 9°35′0.00″E) is located in Douala, Cameroon, along the Atlantic coast of West Africa (Fig. 1). The Wouri Estuary consists of ~1500 km^2 of open water and ~1800 km^2 of mangrove forest (Fossi Fotsi et al., 2019; Gabehe and Smith, 2002; Ndongo et al., 2015; Simon and Raffaelli, 2012). The mangrove forest in the Wouri Estuary is part of the ~180, 000–200,000 ha of coastal mangrove forest that extends from the Rio del Rey Estuary to the west of Mt. Cameroon to the mouth of the Sanaga River to the east (Ajonina et al., 2008; Din et al., 2002; Zogning, 1993). The coastal mangroves which have more than 30 species of mangroves are dominated by red mangroves (*Rhizophora racemosa; Rhizophora harrisonii; Rhizophora mangle (Rhizophoraceae),* white mangroves (*Avicennia germinans (Avicenniaceae); Laguncularia racemosa*) and *conocarpus erectus* (Jean-Hude et al., 2016; Nfotabong-Atheull et al., 2013; Zogning, 1993).

The climate of the estuary and surrounding region is tropical monsoon (Peel et al., 2007) with a long rainy season from March to November and a short dry season from December to February. The wettest months of the year are June, July and August. Between 1982 and 2012, the average annual rainfall was 3702 mm and the annual average temperature was 26.2 °C (Climate-Data.org, 2020). Humidity remains high at an absolute maximum of around 100% throughout the year (Din et al., 2002). The wind speed is generally low except during setting phases of the Saint Helene anticyclone from March to April.

Three major rivers flow into the Wouri Estuary. The Wouri River enters the estuary at its head, while at about 18 km from the estuary mouth, the Mungo River drains into the estuary from the west and the Dibamba River drains into the estuary from the east (Gabehe and Smith, 2002, Fig. 1). River runoff into the estuary is 40 x 10^6 m^3/d from the Wouri River with a catchment of ~8250 km^2, 60 x 10^6 m^3/d from the Mungo River with a catchment of 4200 km^2 and 40 x 10^6 m^3/d from the Dibamba River with a catchment of 2400 km^2 (Gabehe and Smith, 2002). Numerous tidal creeks cut through the mangrove forest, connecting the mangrove forest to the open water of the estuary, the Mungo River and the Dibamba River (Fig. 1). The mean salinity is relatively low at less than 25% of seawater in the estuary (Din et al., 2002). The dilution rate is very high such that during the rainy season, the salinity in estuarine mangroves is zero in less than 30 km away from the ocean (Din et al., 2002). The tidal rhythm in the estuary is semi-diurnal with tidal ranges changing from mesotidal (values $>$ 2 m) to microtidal (values $<$ 2 m) (Onguene et al., 2014). The estuary is depicted as hypersynchronous, meaning that the tidal amplitude progressively increases towards the upper estuary such that the maximum amplitude value is reached at 30 km away from the mouth of the estuary (Allen et al., 1980). During a single tidal cycle, the tidal wave can propagate more than 60 km upstream from the mouth of the estuary (Olivry, 1974).

The estuary has a low-lying relief with altitude ranging from 3 to 100 m above sea level (Willy, 2016). The maximum depth of the estuary after dredging is 25 m (i.e., along the harbor channel) and reduces to 6 m around the Bonaberi bridge.

3. Methods

We conducted this study from June 27th to July 2nd, 2019, during peak rainy season when we could capture the maximum effects of tidal and river-induced transport in the hydrologic mixing of the estuary. We deployed Solinst™ LTC (level, temperature, conductivity) leveloggers near the mouth of the Dibamba River (3°56′23.55″N, 9°42′50.25″E), in a tidal creek (3°57′58.04″N, 9°41′39.22″E) in the mangrove forest (Mangrove Creek) mid-estuary and a tidal creek (4°0′4.20″N, 9°42′3.40″E) and a tidal creek along the shoreline (Dr. Creek) near the head of the estuary (Fig. 1). The water level sensor of the Solinst™ LTC records water level with an accuracy of ±0.1% percentage of full scale

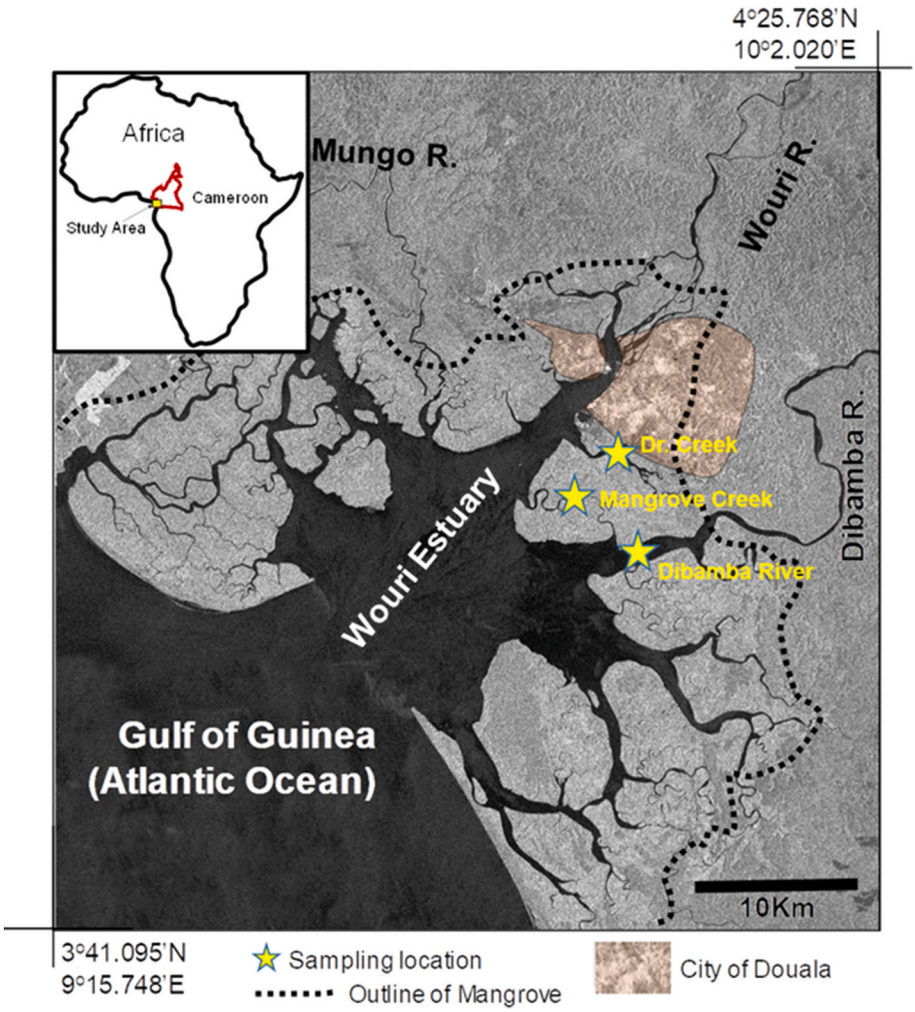

Fig. 1. Map of the Wouri Estuary in Douala, Cameroon, West Africa (insert shows map of Africa and the location of the Wouri Estuary in Cameroon). Also shown are locations where data loggers were deployed at the mouth of the Dibamba River, a tidal creek (Mangrove Creek) in the mangrove at mid estuary and a tidal creek (Dr. Creek) at the estuary head.

with an automatic compensation range from 10 °C to 40 °C. The 4-electrode conductivity sensor of the Solinst™ LTC has a resolution of 1 μS, with ability to measure on a full range of 0–80,000 μS/cm and can operate in temperatures from −20 °C to 80 °C. We also deployed a Solinst™ barologger to record the air temperature (°C) and the barometric pressure (kPa). The accuracy of the air temperature sensor is ±0.05 °C with a resolution of 0.003 °C and the accuracy of the barologger pressure sensor is +0.05 kPa. The Solinst™ LTC leveloggers and the barologger were set to an altitude of 0 m above sea level (a.s.l) and were programmed to collect data in a linear sampling mode at minute intervals from June 27 to July 02, 2019.

The data from the Solinst™ LTC leveloggers and the barologger were downloaded into Microsoft Excel™ where processing and analysis was done. We corrected the water levels recorded by the leveloggers for barometric pressure variations by subtracting the time equivalent barometric pressure values recorded by the barologger. The specific conductance recorded by the leveloggers were converted to salinity using empirical data: (Salinity = 0.0006 x Specific Conductance (μS/cm) - 0.082; $R^2 = 0.998$) (e.g., Bennett, 1976) from simultaneous measurements of specific conductance and salinity made by us in the estuary.

4. Results

4.1. Variations in tides

The tidal time series recorded as variations in water levels at all three locations show similar cyclical patterns and differ slightly in peak arrival times by 35 min between the river mouth station and the mangrove creek station and 51 min between the river mouth station and shoreline creek station. The tidal ranges were above 1.5 m, with the highest range of 2.2 m observed at the mangrove creek station. Tidal ranges measured at the river mouth station and the shoreline creek stations were 1.6 m and 2.1 m, respectively (Table S1). Tidal variations indicate semidiurnal mixed tides (Fig. 2a, b and c).

4.2. Variations in salinity

During this study, the range in salinity at the river mouth, mangrove creek and shoreline creek stations are 4.3, 2.1 and 0.6 psu, respectively (Table S1). The temporal response in salinity at all three stations show cyclical patterns with variations in amplitude responses (Fig. 2d, e and 2f). The cyclicity of the high and low salinity values at the river mouth (Fig. 2d) and the mangrove creek (Fig. 2e) mimicked tidal behavior (Fig. 2a and b). At the river mouth, the salinity peaks are sharp, whilst the salinity troughs are flat (Fig. 2d), whereas for the mangrove creek, the salinity peaks and troughs are similarly flattened or sub-rounded. At

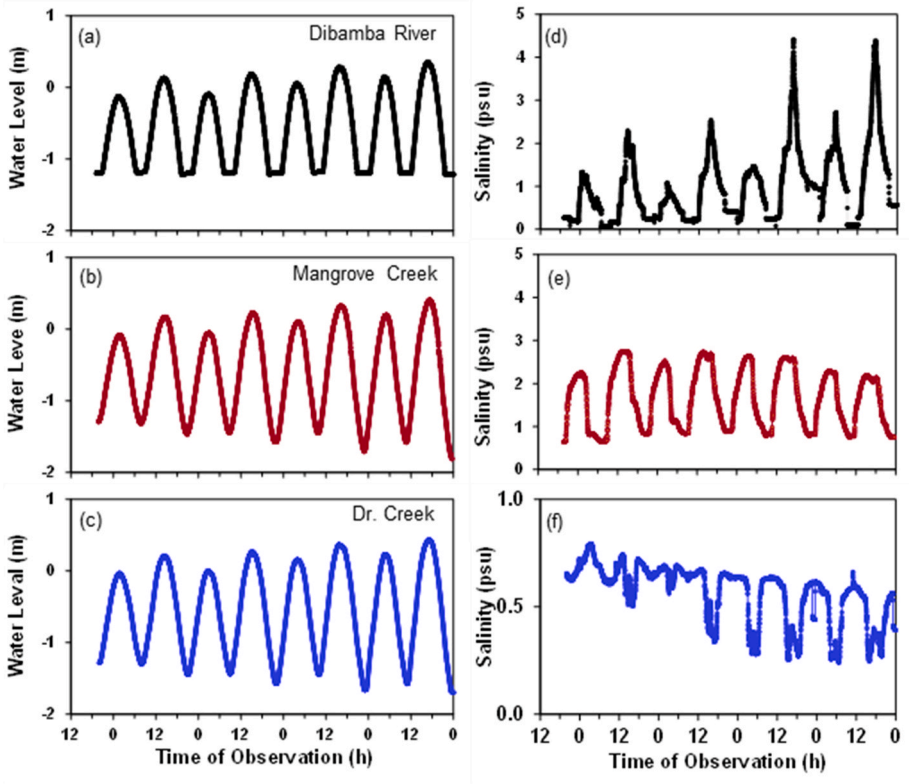

Fig. 2. Time series variations in water levels (tides) at (a) the mouth of the Dibamba River, (b) Mangrove Creek and (c) Dr. Creek and salinity at the mouth of (d) the Dibamba River, (e) Mangrove Creek and (f) Dr. Creek.

the river mouth, the salinity continuously increased in magnitude with time (Fig. 2d). In the mangrove creek, the salinity peaks were either sub-rounded or flat, whereas the salinity troughs were characterized by variable widths (Fig. 2e). The troughs sometimes showed minor flat segments before the salinity decreased to the lowest value (Fig. 2e). The trend in salinity for shoreline creek (Fig. 2f) is out of phase with that of the river mouth (Fig. 2d) and mangrove creek (Fig. 2e). The trend in salinity for shoreline creek is characterized by higher salinity at low tides and lower salinity at high tides (Fig. 2f). The salinity peaks at low tides are either flat or rounded. At high tides, the salinity troughs show minor salinity peaks. Over time, we observed progressive decrease in salinity at high tides and at low tides.

5. Discussion

5.1. Model of hydrologic mixing and salinity responses at different locations in mangrove estuaries

Three important variables control salinity changes during mixing in an estuary (1) tidal forces which primarily impact water movement through flooding and ebbing, (2) initial salinity of the end member waters being mixed (e.g., seawater and freshwater) and (3) the relative volume of the water from different sources (seawater, river water, groundwater, or rainwater). It is worth noting that tidal forces can be decoupled from water salinity which is concentration dependent and from water volume which depends on hydrologic factors such as river discharge and tidal volume. Therefore, tidal forces that primarily control the movement of water in an estuary may not necessarily change the salinity of the water equally at all locations.

Models of estuarine mixing often describe two distinct end members: freshwater and seawater. For this two-end member mixing during tidal flooding and ebbing, the change in salinity typically relates to the proportion of seawater and freshwater because salinity is conservative (e.g., Fry, 2002; Lewis, 1980; Loder and Reichard, 1981). Thus, to compare changes in salinity over the same tidal cycle in different locations of a mangrove estuary, we can normalize for tides using water levels measured at each location. The normalization of tides is given by:

$$NL = (L_i - L_{min})/L_{max} - L_{min}) \quad (1)$$

where NL is the normalized water (tide) level, L_i is the instantaneous water level at a given time, L_{min} is the minimum water level (low tide) and L_{max} is the highest water level (high tide). Conservative end member mixing of seawater and freshwater based on salinity can be described for different locations in a mangrove estuary using normalized tides vs. salinity behavior.

5.1.1. Mixing by seawater intrusion depicted by normalized tide-salinity plots

A model of normalized water level vs. salinity (tide-salinity) behavior for a location in an estuary where there is mixing with intruding seawater is shown in Fig. 3a. If the salinity of the intruding seawater during high tide (open circle, Fig. 3a) is the same as that present in the estuary at low tide (filled circle, Fig. 3a), then mixing will follow the path shown by Line 1, which shows no salinity changes during a full tidal cycle of flooding and ebbing. If the salinity of the intruding seawater during high tide (hatched circle, Fig. 3a) is higher than that in the estuary at low tide, then during tidal flooding and tidal ebbing, the seawater and estuarine water mix according to Line 2 and Line 4 (Fig. 3a) that depict linear mixing. Line 3 depicts mixing at a measuring station during flooding where seawater located between the measuring station and the seawater (high tide front) is mixed and transported past the station, followed by mixing with seawater to peak tide. In this scenario, the residual water in the estuary has a linear salinity gradient which between tides, depends on the tidal exchange volume. During the start of tidal ebbing, withdrawal of seawater from high tide that mixed with freshwater upstream of the measuring station will be characterized

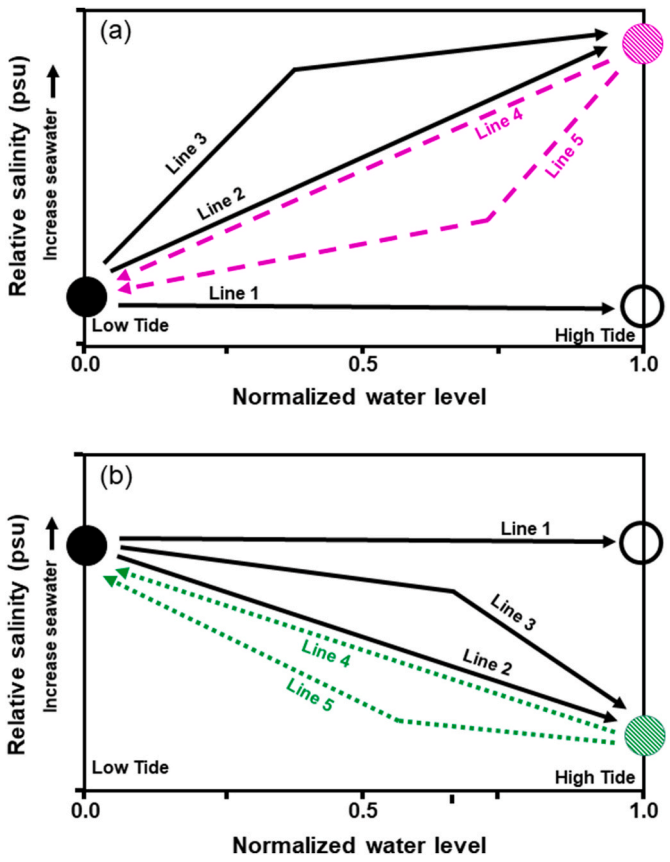

Fig. 3. Cross plot of normalized water level vs. relative salinity for (a) seawater mixing and (b) freshwater mixing. The arrowed solid lines show direction of mixing during tidal flooding and the arrowed dashed lines show mixing during tidal ebbing.

by a rapid salinity decrease shown by steeper slope in Line 5 near high tide (Fig. 3a). When the ebbing front recedes past the measuring station, mixing is dominated by freshwater characterized by a slower rate of salinity decreasing to low tide depicted by the rest of Line 5.

5.1.2. *Mixing of freshwater depicted by normalized tide-salinity plots*

A model of tide-salinity behavior for a location in an estuary where there is mixing with freshwater discharged from a river is shown in Fig. 3b. Line 1 shows mixing between residual estuarine water shown as a filled circle at low tide with incoming river water that has the similar salinity shown as an open circle at high tide. During tidal flooding and ebbing, linear mixing between estuarine water shown as a filled circle at low tide and freshwater shown as a hatched circle at high tide is depicted by Line 2 and Line 4, respectively (Fig. 3b). Line 3 depicts the mixing of lower salinity water between a measuring station and the freshwater front, followed by freshwater mixing, evidenced by the subsequent dilution/freshening to peak tide. During tidal ebbing, mixed freshwater upstream of the measuring station is transported past the measuring station, followed by mixing with more seawater causing the salinity to return to background values as depicted by Line 5.

5.1.3. *Interpreting seawater-freshwater mixing from tide-salinity plots*

Mixing models based on normalized tide-salinity plots have value in illustrating the extent of variations in the proportions of mixing water sources at different locations in a mangrove estuary. In the conceptual model of mixing of seawater and freshwater (Fig. 3a), the mixing trajectory that characterize two end members mixing with similar salinity are depicted by Line 1. This can be described as *suppressed* salinity change. The trajectories that illustrate the salinity changes during the mixing of waters with contrasting salinity, as tides vary, are depicted by Line 2 and Line 4 (Fig. 3a and b). The trends in Fig. 3a shows increasing salinity, which is normally expected, i.e., *normal* salinity change and Fig. 3b shows decreasing salinity, which is contrary to expectations, i.e., *reverse* salinity change. Mixing between two end members with contrasting salinity, followed by further mixing with a third end member with a different salinity is depicted by Line 3 and Line 5 (Fig. 3a and b). The conceptual model shows that hydrologic mixing in an estuary can be captured in the trends of tide-salinity plots in situations where the salinity of the "masses of water" that mix are markedly different, and the mixing is sequential.

5.1.4. *Conceptualizing hydrologic mixing in the Wouri Estuary*

The Wouri Estuary has an upper river source along its longitudinal axis and two river sources on both sides of this axis about 18 km from its river mouth (Fig. 1). Thus, the hydrologic mixing dynamics in the upper estuary and along the longitudinal axis is likely to be different from that of a typical (single river) estuary. This is because of the additional sources of freshwater discharged into the estuary. Furthermore, the Wouri estuary has a mangrove forest which can affect the hydrology and salinity changes in mixing between water from the open estuary and that in the mangrove forests. We use the recent model of the tidal freshwater zone (TFZ) by Jones et al. (2020) as the basis for interpreting the hydrologic mixing dynamics in the Wouri Estuary (Fig. 4). In this model, the tidal and river forces are used to delineate major regions in the estuary including the TFZ (see Jones et al. (2020) and references therein for details). The four salinity-based zones from the ocean towards and beyond the estuary head are (1) tidal saline zone beyond the estuary mouth, (2) tidal brackish zone (segment a), (3) tidal freshwater zone (TFZ) (segments b and c) and (4) the non-tidal river zone (segment d). Although the entire estuary is affected by tide-induced oscillations of the surface water stage, the basis used for segmenting the TFZ is the river flow direction which is bi-directional in segment b and unidirectional in segment c. The schematic in Fig. 4, shows the three main rivers entering the main estuary channel with the Wouri River (WR) at the head, the Mungo River (MR) to the left and the Dibamba River (DR) to the right in the mid-estuary. We show the sampling locations in the Dibamba River, the mangrove tidal creek (MC) and the shoreline Dr. Creek (DC) (Fig. 4), based on their temporal salinity (see Fig. 2d, e and f). Although the tidal saline, tidal brackish, TFZ and the non-tidal river zones are well defined in this schematic, they are not necessarily stationary in space and time because some zones can merge and/or get eliminated depending on two extreme conditions (i.e., river dominance vs. estuarine dominance) as the riverine and tidal forces change in space and time (Jones et al., 2020).

5.2. *Hydrologic mixing at the river mouth, mangrove creek and shoreline creek from normalize tide -salinity patterns*

The water level response corresponding to tides at the mouth of the Dibamba River, Mangrove Creek and shoreline Dr. Creek are similar (Fig. 2a, b and c), but their salinity behavior is markedly different over eight sequential semidiurnal mixed tides (Fig. 2d, e and f). The tide-salinity plots of normalized water level for the eight sequential semidiurnal mixed tides are shown in Fig. 5. The plots in Fig. 5 show the salinity behavior during tidal flooding in blue, whilst the salinity behavior during tidal ebbing are shown in green.

In general, the salinity changes during tidal flooding and ebbing reveal characteristically distinct saline water-freshwater mixing from hysteresis (tide-salinity patterns) at each of the three stations (Fig. 5). Additionally, the tide-salinity patterns at each station vary with mixed tides, as the tide magnitude changes with time (top to bottom panel in Fig. 5). The distance that seawater from the Gulf of Guinea travels to reach the mouth of the Dibamba River station is 30 km, 35 km to reach the Mangrove Creek station and 40 km to reach the shoreline Dr. Creek station. Because of this proximity, the timing for high and low tides are

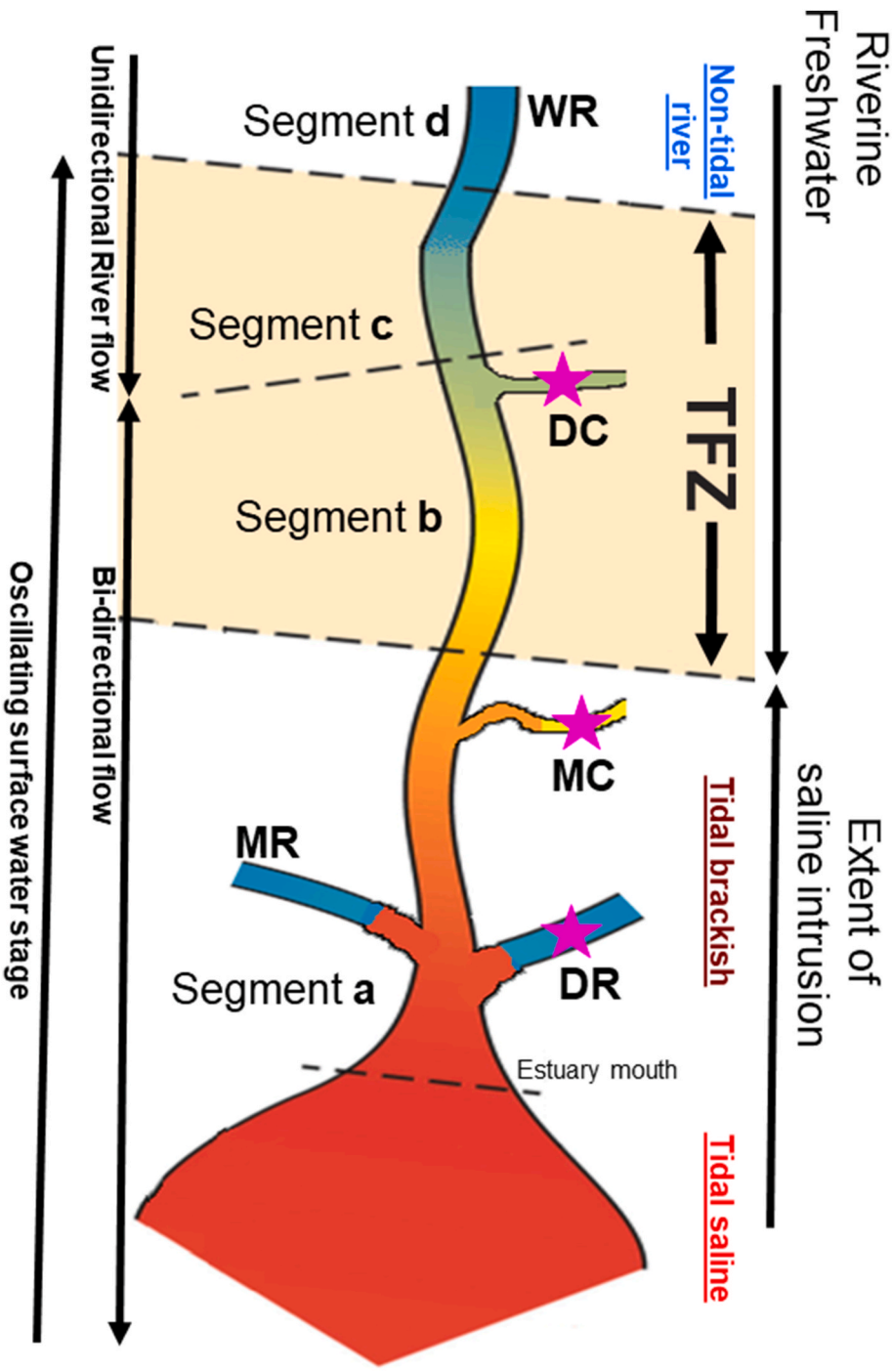

Fig. 4. Schematic of a hypothetical tidal freshwater zone (TFZ) in the Wouri Estuary adapted from Jones et al. (2020). The divide between fresh and brackish water column is between segments a and b, the upstream limit of bidirectional discharge is between segments b and c and the upstream limit of tidal surface water stage fluctuations is between segments c and d (See Jones et al. (2020) for details). DR, MR, WR, MC and DC represent the Dibamba River, Mungo River, Wouri River, Mangrove Creek and Dr. Creek, respectively. Sampling stations are shown as stars.

nearly similar and the spatial distances separating the stations do not constitute a significant variable to explain the tide-salinity patterns observed. The patterns displayed on the normalized tide-salinity plots (Fig. 5) are affected by the hydrologic mixing and can be explained by considering the hydrologic interactions depicted in our conceptual model (Fig. 3) and the spatial location of each station in relation to TFZ of estuary (Fig. 4).

5.2.1. Tide-salinity patterns at the mouth of the Dibamba River

The maximum salinity encountered during mixing in the mouth of the Dibamba River is ~4.4 psu and we consider this sampling station to be located in the tidal brackish zone (Jones et al., 2020, Fig. 4). At the mouth of the Dibamba River, the tide-salinity patterns (Fig. 5a–h) show that the salinity during tidal flooding (data in blue) is lower than the salinity during tidal ebbing (data in green). The panels (Fig. 5a–h) show marked increases in the salinity that starts from ~0.5 to 0.8 normalized tide and another increasing salinity behavior from 0.8 to peak normalized tide, where the salinity increased by as much as 50% (e.g., Fig. 5f). We also note that near the normalized tide peak, the salinity rise varies markedly between sequential tides, perhaps indicating specific mixing behavior at peak rising tide. It is clear that the tide-salinity segments from 0 to <0.8 normalized tide where the salinity is nearly constant (Fig. 5a–h), the end member mixing can be represented by constant salinity end members shown as Line 1, Fig. 3a. The salinity increase observed between a normalized tide of 0.3–0.6, which increases steadily to 0.8 normalized tide, and then increases further to near normalized

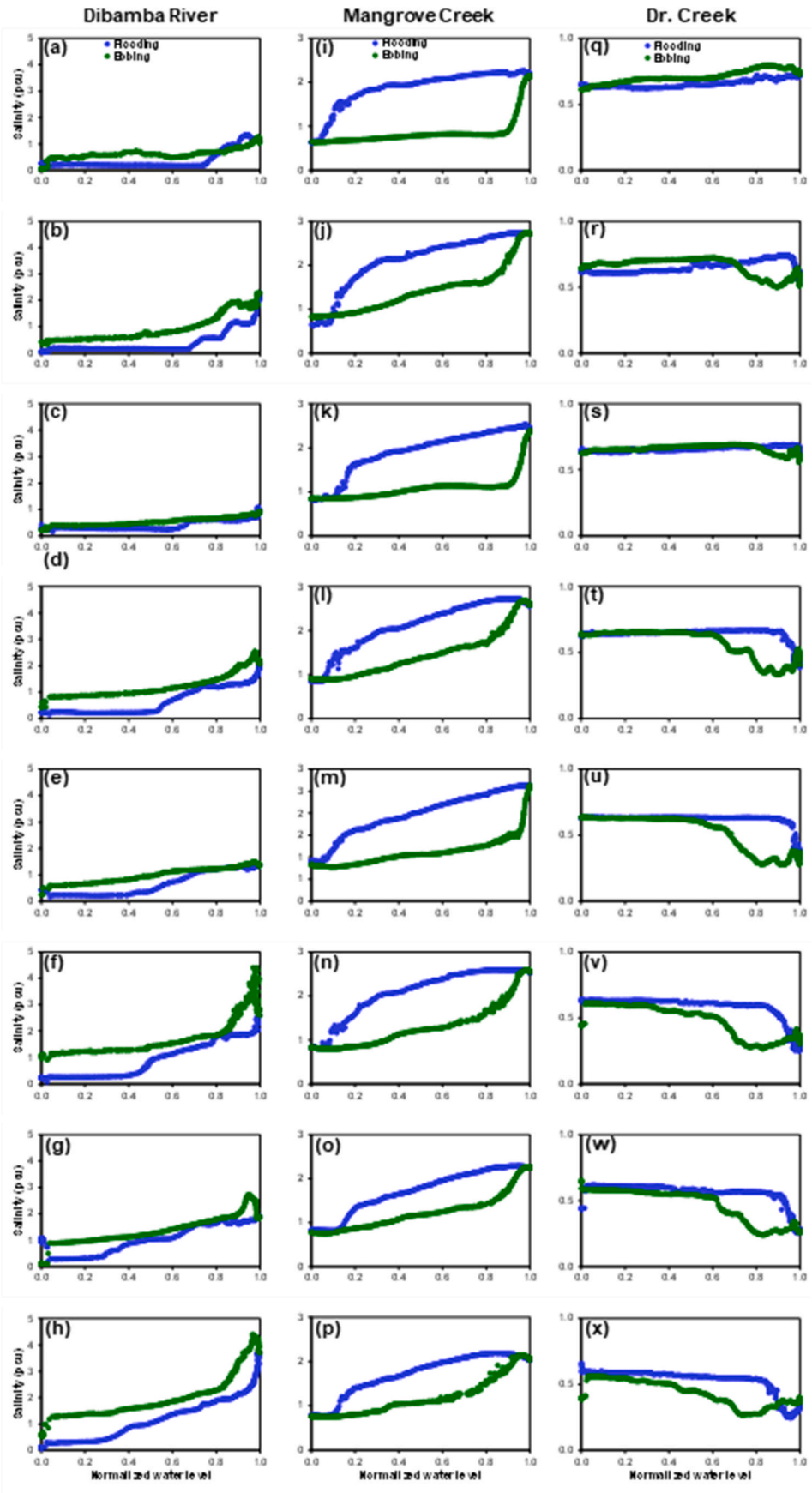

Fig. 5. Cross plots of normalized water levels (tides) vs. salinity at (a–h) the mouth of the Dibamba River, (i–p) Mangrove Creek and (q–x) Dr. Creek.

peak tide, is indicative of seawater intrusion and mixing. The "stepwise" increase in salinity can be explained by the transport of different "packages" of mixed seawater water past the station. During tidal flooding, the tide-salinity patterns at the mouth of the Dibamba River (Fig. 5a–h) is best described by sequential seawater mixing by combining Line 1 and variations of Line 3, as demonstrated in our conceptual model for seawater mixing (Fig. 3a).

The salinity regime during tidal ebbing shows the recovery from seawater intrusion, marked by a salinity decrease of more than 50% from normalized peak tide to ~0.8 normalized tide (Fig. 5a–h). These marked decreases in salinity are followed by the slow decreases of salinity to near low (0.1 normalized) tide. The initial rapid decrease in salinity is due to the tidal-controlled transport of the upstream mixed seawater. The rate of transport of the seawater from upstream depends on the balance between the riverine and tidal forces, with shorter transport time from higher riverine forces (or discharge). We speculate that beyond the withdrawal of tide-induced mixed seawater from the river mouth, the slow salinity change to low tide is from drainage of mixed seawater-freshwater from the mangrove forest. This seawater-freshwater mixture is released to the river until near low tide when flow from the mangrove forest is cut off, after which the salinity of the river water returns to that of freshwater (e.g., Fig. 4c). The storage and release of water from the mangrove forest is described as lateral trapping, where water that is temporarily stored in the mangrove forest during tidal flooding, drains and mixes with water in the channel during tidal ebbing (Alongi and Brinkman, 2011; Wolanski and Ridd, 1986; Wolanski et al., 2001). During tidal ebbing, the tide-salinity patterns at the mouth of the Dibamba River (Fig. 4a–h) is described by Line 5 from our conceptual model for seawater mixing (Fig. 3a).

5.2.2. Tide-salinity patterns in a tidal creek in the mangrove forest

The maximum salinity observed at Mangrove Creek is ~2.7 psu, and we consider this sampling station to be located in the upper tidal brackish zone (Jones et al., 2020, Fig. 4). At the Mangrove Creek (Fig. 5i-p), the tide-salinity patterns show that the salinity during tidal flooding (data in blue) is always higher than the salinity during tidal ebbing (data in green). The panels (Fig. 5i-p) show that during tidal flooding, there is little change in the salinity between 0 and 0.1 normalized tide, after which there is a marked increase in the salinity between 0.1 and ~0.2 normalized tide, which is followed by a continuous increase in salinity to peak normalized tide (e.g., Fig. 5m). The stepwise tide-salinity trajectory indicates hydrologic mixing with at least three different "packages" of water with different salinities. It is clear from the nearly flat tide-salinity pattern between 0 and 0.1 normalized tide that mixed seawater transported past the station is water that resides (residual water) in the creek during low tide. As the tides rise, the transport of the residual water past the station is followed by water of slightly higher salinity between 0.1 and 0.2 normalized tide. We speculate that the more seawater transported into the creek is from the main estuary, as longitudinal salinity gradients are reported for tidal creeks draining mangrove forest (Alongi and Brinkman, 2011; Wolanski and Ridd, 1986). Between a normalized tide of 0.2 to peak normalized tide, the seawater is from seawater intrusion. The behavior of the salinity regime during tidal flooding in Mangrove Creek is from sequential mixing of seawater depicted by Line 1, followed by variable combinations of Line 3 as shown in our conceptual model of seawater mixing (Fig. 3a). We infer that at this station, the tide-salinity patterns document transport of water between the main estuary and mangrove forest, as well as indicate seawater intrusion from rising tides.

The tide-salinity patterns during tide ebbing show a marked decrease in the salinity by more than 50% from maximum normalized tide to ~0.8 normalized tide, which is followed by a gradual decrease in salinity to the lowest salinity at low tide (Fig. 5i-p). The initial decreases in salinity from maximum normalized tide to ~0.8 normalized tide during tidal ebbing are characterized by variable slopes, and indicate the transport of variably diluted seawater near peak normalized tide. It is not clear what the source of this less saline water is, but we speculate that it is likely water drained from the mangrove forest, and therefore points to freshwater dilution of seawater (saline water) in the mangrove forest. The Wouri Estuary and the region receive about ~350 mm monthly (~12 mm/d) rainfall in June (Climate-Data.org, 2020), which is the period when we conducted this investigation. We posit that the rainwater trapped on the mangrove forest platforms diluted the mixed seawater delivered at high tide to cause the observed salinity dilution at the start of tidal ebbing (Din et al., 2017; Drexler and Eric, 2002; Hayes et al., 2019; Kjerfve et al., 1999; Komiyama et al., 2020; Krauss et al., 2007). Additionally, different amounts of rainwater trapped on the mangrove platforms may explain the variability of the slope of the diluted seawater at the start of tidal ebbing (e.g., Fig. 4m vs. 4n). It is also important to note that the variable dilution occurs at the scale of the tidal cycle. Dilution can also occur from fresh submarine groundwater discharge (SGD) spatially across estuaries. Assuming fresh(er) SGD in the mangrove forest, it is possible that the rate of discharge is sufficiently high to dilute the mixed seawater transferred to the mangrove platforms and the creek at high tide and before tidal ebbing (Drexler and Eric, 2002; Hayes et al., 2019; Mazda and Ikeda, 2006). Additionally, variability of SGD could also explain the variable dilution at the tidal cycle scale. The cause of the slow decrease in salinity between 0.8 normalized tide to low tide can be explained by drainage of water from the mangrove forest associated with lateral trapping (Alongi and Brinkman, 2011; Wolanski and Ridd, 1986; Wolanski et al., 2001). This is similar to the slow salinity decrease observed for the Dibamba River during tidal ebbing (Fig. 5a–h). Irrespective of the mechanism of seawater dilution during tidal ebbing at the Mangrove Creek station, the tide-salinity patterns capture a salinity regime that can be described by hydrologic mixing depicted by Line 5 in the normalized tide-salinity conceptual model for seawater mixing (Fig. 3a).

5.2.3. Tide-salinity patterns in a tidal creek at the estuary head

The maximum salinity measured in shoreline Dr. Creek was 0.8 psu, which we use to locate Dr. Creek in the upper region of segment b in the TFZ (Jones et al., 2020, Fig. 4). In Dr. Creek, the tide salinity patterns (Fig. 5q–x) show that during tidal flooding (data in blue), the salinity is nearly constant from 0 to 0.9 normalized tide, then the salinity decreases to peak normalized tide. We note that at near peak normalized tide, the salinity increases before tidal ebbing begins (e.g., Fig. 5u), creating characteristic tide-salinity patterns that vary over time both in shape and duration, indicating unique mixing behavior at peak tide.

During tidal flooding, the nearly constant salinity as normalized tides increase from 0.0 to ~0.9 indicate the absence of seawater intrusion into the creek during tidal flooding (e.g., Fig. 5u). This behavior of constant salinity during tidal flooding can be explained by mixing with water of similar salinity between the station and the estuary transported past the station. The constant salinity is depicted by mixing shown by Line 1 in our conceptual model for freshwater mixing (Fig. 3b). The tide-salinity patterns from ~0.9 to near peak normalized tide, where the salinity decreased must be due to freshwater mixing (less seawater compared to water in the creek), which can be depicted by freshwater mixing behavior similar to Line 3 near peak tide (Fig. 3b). We presume that the slightly higher salinity observed at the shoreline Dr. Creek station at peak tide (Fig. 2f) is from seawater intrusion. Therefore, we explain the freshwater mixing phenomena between 0.9 and near maximum normalized tide by "hydraulic blockage" of Wouri River flow by rising tide, which causes river water to flow laterally into the tide channels, inducing dilution to near high tide. By peak tide, the rising tide front propagates into the estuary head past the mouth of the tidal creek. As the rising tide front advances past the mouth of the shoreline Dr. Creek, the mixed seawater from the estuary flows into the tidal creek past the station, albeit, only briefly to cause the salinity rise at peak normalized tide. We note that the temporal variability of the effects of mixed tides manifest in the absolute salinity change, and on the tide range during which dilution occurs (e.g., Fig. 5s vs. 5t).

As the tides ebb from peak tide to ~0.9 normalized tides, the salinity decreases from the salinity maximum to lower salinity values (Fig. 5q–x). The salinity then increased to higher values between ~0.7 and 0.3 normalized tides. In fact, the increase in salinity can be very rapid (e.g., Fig. 5s), can rise and exceed that of the salinity during tidal flooding (e.g., Fig. 5r) or may actually be higher than that of tidal flooding throughout the ebb tidal cycle (e.g., Fig. 5q). We suggest that the tide-salinity pattern from peak tide to 0.7 normalized tide indicates freshwater transported past the station during the start of tidal ebbing. The slow salinity increases to maximum salinity between normalized tides of 0.7 and 0.3 occurs in a tidal range that is much broader compared to that of dilution during tidal flooding (e.g., Fig. 5x). In other words, the freshening during tidal flooding was more abrupt compared to the slow salinization to background salinity. The normalized tide-salinity pattern observed during tidal ebbing can be characterized by sequential mixing of more seawater depicted by Line 5 and followed by Line 1 shown in our conceptual model for freshwater mixing (Fig. 3b). The stepwise increase in the salinity during tidal ebbing may indicate different "packages" of mixed seawater (saline water) withdrawing past the station. The salinity variations of these packages of water also indicate that they are unlikely the same water packages that were transported past the station during tidal flooding. It took a change of 0.1 normalized tide during flooding to cause freshening at the station (e.g., Fig. 5u). Although variable, the freshening lingered in the creek from peak tide to ~0.7 normalized tide, which is more than twice the normalized tide value during flooding to freshen the tidal creek water (e.g., Fig. 5u). The semidiurnal mixed tides in the Wouri Estuary do not explain both the duration of withdrawal of freshwater and the observed stepwise salinity behavior. We suggest that there was more freshwater being withdrawn past the station during tide ebbing than was delivered during tidal flooding. The salinity of the water during tidal ebbing was higher than that of the creek at low tide, and thus, has a different source from river water transported from the estuary to the tidal creek.

The normalized tide-salinity patterns during tidal ebbing indicated that the water in the shoreline Dr. Creek is less fresh, compared to river water, which invaded the creek near high tide (Fig. 2c; Fig. 5q–x). One source of the slightly higher salinity water input into Dr. Creek is likely SGD. Dr. Creek is the furthest tidal creek located along the shoreline near the headwater of the Wouri Estuary. Although Dr. Creek was previously bounded by freshwater marshes to the north and mangrove forest to the south (see Fig. 1), the marshes have been destroyed and are now a built-up urban environment (Din et al., 2017). Nevertheless, the shoreline Dr. Creek represents the limit of the estuary, and is at the interphase where groundwater likely discharges to the estuary. Groundwater in the coastal aquifer along the shoreline Dr. Creek has a salinity of about 1 psu (Ramatlapeng et al., 2021), and its discharge into Dr. Creek will cause the salinity to be higher than that of the Wouri River discharging in the headwater of the estuary and may be responsible for the slow salinity increase to low tide in the shoreline tidal Dr. Creek.

6. Implications and limitations

Tropical estuaries and their mangrove forests along the African coast constitute a heterogeneous environment (e.g., Allersma and Tilmans, 1993) with salinity and hydrology varying over short to long temporal scales. Tide-salinity patterns constructed from normalized tides vs. salinity are a useful way to characterize seawater-freshwater mixing dynamics and to elucidate the processes that control salinity in spatially different regions of estuaries with mangrove forest complexes (e.g., Fig. 5). The water sources and hydrologic mixing processes at the mouth of a river, a tidal creek in a mangrove forest midway in an estuary and in a tidal creek at the shoreline near the head of an estuary were determined using tide-salinity patterns. The tide-salinity patterns are able to characterize different "packages" of water that mix and the order in which the mixing occurs relative to the timing and duration of tides. Additionally, there is marked variability in the tide-salinity patterns when the tides transition from flood to ebbing and vice versa (Fig. 2d, e and f; Fig. 5) which are characteristics for each tidal cycle at each investigated site.

The hydrologic mixing behavior at the same station (Fig. 5a–h, 5i-p and 5q-x) showed temporal changes either because of the shift in the sources of water or proportions of different waters that mix, or the temporal riverine and tidal forces-imposed change on the hydrologic regime. Thus, the tide-salinity patterns allow for comparison amongst different locations in an estuary (e.g., open water, mangrove forest, river mouth in this study) and for the assessment of the temporal evolution salinity (reflecting the biogeochemistry) at the different locations. Because our study was conducted only briefly in time (over 4 days) and during the peak of the rainy season (June), it does not characterize the range of tide-salinity patterns possible at each study location. This is because the balance between the tidal and riverine forces change at the event level (e.g., storm events) and through tidal cycles and seasonal cycles (Jones et al., 2020). Thus, changing riverine and tidal forces will require tide-salinity patterns to be constructed for all changing conditions to fully capture the range of tide-salinity patterns for locations of interest.

If we are interested in biogeochemical reactions and hydrochemical changes in estuarine systems, then their temporal reaction scale (Langmuir, 1997) dictates how often we should sample to measure the water properties of interest. Efficient experiments to decipher processes must be designed to capture changes in parameters that can be used to assess the process(es) effectively. For example, in the shoreline tidal creek near the estuary head, an experiment designed to capture the processes that control salinity during a tidal cycle should have a sampling protocol in which the sampling frequency during tidal flooding is different from that of during tidal ebbing. A sampling interval that does not increase disproportionately over the tidal duration will not capture the brief freshening and salinity increase near the peak of the flood tide (e.g., tide salinity pattern in Fig. 5u). A sampling interval designed to capture processes during tidal flooding may need to be modified to capture processes during tidal ebbing, as the duration of the process(es) controlling water salinity are different (e.g., Fig. 5u). The same can be said for the tidal creek in the mangrove in the mid-estuary and at the river mouth, where the rate of change of salinity can only be captured by prior knowledge of the behavior revealed by the tide-salinity patterns (Fig. 5a–h; 5i-p).

If flushing time in different parts of the estuary and mangrove forest need to be known, the tide-salinity patterns are instructive. Using the tide-salinity patterns, flushing time based on salinity concentrations can be directly observed at different temporal scales (e.g., Fig. 5). Additionally, if observed spatially across the open water and mangrove forest, different locations can be classified based on observing the flushing time at the location and the processes that control the hydrologic and biogeochemical processes during the tidal cycles can be investigated.

Finally, the temporal tide-salinity regime also records the temporal changes in processes. It is clear from our results that in a semidiurnal mixed tide estuary, the variable tide conditions are captured in the tide-salinity patterns (compare Fig. 5a vs. b vs. c vs. d; Fig. 5i vs. j vs. k vs. l; Fig 5q vs. r vs. s vs. t). Our results can be used to suggest that spring and neap tide regimes, as well as variation in freshwater (river) discharge associated with seasonal and annual discharge will affect the tide-salinity patterns.. Therefore, establishing tide-salinity patterns for a location over sub-tidal cycles to seasonal scales or longer can define the expected variations in seawater-freshwater mixing, and can guide long-term studies of biogeochemical processes. We speculate that over the longer term, tide-salinity patterns can also provide insights on the effect of sea level rise across space in estuaries and mangrove forests.

7. Conclusions

A time-series investigation of water level (tides) and salinity at the mouth of a river and two tidal creeks in the tropical Wouri Estuary in

Douala, Cameroon showed distinct tidal and salinity responses at each location. The salinity variation during tidal flooding and tidal ebbing were defined by hysteresis, consistent with an idealized conceptual model depicting either mixing of seawater and freshwater, mixing of seawater with residual mixed seawater or mixing of freshwater and residual mixed seawater. In our conceptual model, hydrologic mixing in estuaries is defined by linear segments in the tide-salinity space. The hydrologic and salinity mixing trajectories revealed by the tide-salinity patterns are unique at each station and the variations in the tide-salinity trajectories indicate changing tidal and river forcing, as well as and the effects of tidal and river induced transport on hydrologic mixing. Our results show that the tide-salinity patterns for one tidal cycle in this semidiurnal mixed tide estuary is adequate to define the gross hydrologic behavior at each location. Our results also show that tide-salinity patterns over multiple tidal cycles are needed to characterize hydrologic mixing related to a combination of varying tidal and riverine forces and their effects on the varying topographic landscape of mangrove estuaries.

We suggest that the temporal (time series) salinity changes can be used to determine the temporal behavior and exchange of water between the open water in an estuary and mangrove forests via tidal creeks, which is essential for assessing the salinity regime, biogeochemical processes and pollution abatement. Finally, our results show that the use of the conductivity, temperature and depth (CTDs) for constructing normalized tide-salinity patterns is instructive in determining the spatial and temporal variability of estuarine hydrologic mixing, which is useful for calibrating/verifying the temporal and spatial applicability of salinity-based mixing models.

CRediT authorship contribution statement

Eliot A. Atekwana: Writing- original draft, Supervision, Funding Acquisition, Conceptualization, Methodology. Goabaone J. Ramatlapeng: Writing-reviewing and editing, Data Analysis. Hendratta N Ali: Writing-reviewing and editing, Funding Acquisition. Isaac K. Njilah: Writing-reviewing and editing. Gustave R. N. Ndondo: Writing-reviewing and editing.

Funding

This work was supported by the US National Science Foundation under Grant OISE-1827065.

Declaration of competing interest

The authors declare that they have no known competing financial interests or personal relationships that could have appeared to influence the work reported in this paper.

Acknowledgments

We thank the government of Cameroon (Ministry of Water Resources and Energy) for granting us research permits. We thank the manager and staff of the Aquarius Marina 2000 Hotel for facilitating logistics that made this work possible. We thank the students participating in the US National Science Foundation International Research Experience for Students 2019 field season for help in data acquisition. We thank the anonymous reviewer whose comments helped improve this manuscript.

Appendix A. Supplementary data

Supplementary data to this article can be found online at https://doi.org/10.1016/j.jafrearsci.2022.104684.

References

Allen, G.P., Salomon, J.C., Bassoullet, P., Du Penhoat, Y., De Grandpre, C., 1980. Effects of tides on mixing and suspended sediment transport in macrotidal estuaries. Sediment. Geol. 26 (1–3), 69–90.
Allersma, E., Tilmans, W.M., 1993. Coastal conditions in West Africa—a review. Ocean Coast Manag. 19 (3), 199–240.
Ajonina, G., Diamé, A., Kairo, J., 2008. Current Status and Conservation of Mangroves in Africa: an Overview, vol. 133. World Rainforest Movement Bulletin.
Akamatsu, Y., Ikeda, S., 2016. Surface and subsurface water coupled ecological model in a mangrove swamp, Ishigaki Island, Japan. J. Hydro Environ. Res. 11, 146–159.
Alongi, D.M., Brinkman, R., 2011. Hydrology and biogeochemistry of mangrove forests. In: Forest Hydrology and Biogeochemistry. Springer, Dordrecht, pp. 203–219.
Augustinus, P.G., 1995. Geomorphology and sedimentology of mangroves. Dev. Sedimentol. 53, 333–357 (Elsevier).
Bennett, A.S., 1976. Conversion of in situ measurements of conductivity to salinity. Deep Sea Res. Oceanogr. Abstr. 23 (2), 157–165 (Elsevier).
Brown, N.L., Hamon, B.V., 1961. An inductive salinometer, 1953 Deep Sea Res. 8 (1), 65. IN8.
Climate-Dataorg, 2020. Douala Climate (Cameroon). https://en.climate-data.org/africa/cameroon/littoral/douala-890444/. (Accessed 30 July 2020).
Din, N., Priso, R.J., Kenne, M., Ngollo, D.E., Blasco, F., 2002. Early growth stages and natural regeneration of Avicennia germinans (L.) Stearn in the Wouri estuarine mangroves (Douala-Cameroon). Wetl. Ecol. Manag. 10 (6), 461–472.
Din, N., Ngo-Massou, V.M., Essomè-Koum, G.L., Ndema-Nsombo, E., Kottè-Mapoko, E., Nyamsi-Moussian, L., 2017. Impact of urbanization on the evolution of mangrove ecosystems in the Wouri River estuary (Douala Cameroon). In: Coastal Wetlands: Alteration and Remediation. Springer, Cham, pp. 81–131.
Dubuc, A., Collins, G.M., Coleman, L., Waltham, N.J., Rummer, J.L., Sheaves, M., 2021. Association between physiological performance and short temporal changes in habitat utilisation modulated by environmental factors. Mar. Environ. Res., 105448
Drexler, J.Z., Eric, W., 2002. Source water partitioning as a means of characterizing hydrologic function in mangroves. Wetl. Ecol. Manag. 10 (2), 103–113.
Fossi Fotsi, Y., Pouvreau, N., Brenon, I., Onguene, R., Etame, J., 2019. Temporal (1948–2012) and dynamic evolution of the Wouri estuary coastline within the Gulf of Guinea. J. Mar. Sci. Eng. 7 (10), 343.
Fry, B., 2002. Conservative mixing of stable isotopes across estuarine salinity gradients: a conceptual framework for monitoring watershed influences on downstream fisheries production. Estuaries 25 (2), 264–271.
Gabehe, C.E., Smith, V.S., 2002. Water, salt and nutrients budgets of two estuaries in the coastal zone of Cameroon. West Afr. J. Appl. Ecol. 3 (1).
Guerreiro, M.A., Martinho, F., Baptista, J., Costa, F., Pardal, M.Â., Primo, A.L., 2021. Function of estuaries and coastal areas as nursery grounds for marine fish early life stages. Mar. Environ. Res. 170, 105408.
Hayes, M.A., Jesse, A., Welti, N., Tabet, B., Lockington, D., Lovelock, C.E., 2019. Groundwater enhances above-ground growth in mangroves. J. Ecol. 107 (3), 1120–1128.
Jean-Hude, E.M., Gordon, N.A., Mbarga, A.B., Tchikangwa, B.N., 2016. Bumpy road to improved mangrove resilience in the Douala Estuary, Cameroon. J. Ecol. Nat. Environ. 8 (5), 70–89.
Jones, A.E., Hardison, A.K., Hodges, B.R., McClelland, J.W., Moffett, K.B., 2020. Defining a riverine tidal freshwater zone and its spatiotemporal dynamics. Water Resour. Res. 56 (4), e2019WR026619.
Kjerfve, B., Lacerda, L.D., Rezende, C.E., Ovalle, A.R.C., 1999. Hydrological and hydrogeochemical variations in mangrove ecosystems. In: Yanez-Arancibia, A., Lara-Dominquez, A.L. (Eds.), Mangrove Ecosystems in Tropical America: Structure, Function and Management, INECOL (Mexico), IUCN/ORMA (Costa Rica). NOAA/NMFS, Beaufort, NC, USA), pp. 71–81.
Komiyama, A., Poungparn, S., Umnouysin, S., Rodtassana, C., Kato, S., Pravinvongvuthi, T., Sangtiean, T., 2020. Daily inundation induced seasonal variation in the vertical distribution of soil water salinity in an estuarine mangrove forest under a tropical monsoon climate. Ecol. Res. 35 (4), 638–649.
Koné, Y.M., Borges, A.V., 2008. Dissolved inorganic carbon dynamics in the waters surrounding forested mangroves of the Ca Mau Province (Vietnam). Estuarine. Coast. Shelf Sci. 77 (3), 409–421.
Krumme, U., Herbeck, L.S., Wang, T., 2012. Tide-and rainfall-induced variations of physical and chemical parameters in a mangrove-depleted estuary of East Hainan (South China Sea). Mar. Environ. Res. 82, 28–39.
Krauss, K.W., Keeland, B.D., Allen, J.A., Ewel, K.C., Johnson, D.J., 2007. Effects of season, rainfall, and hydrogeomorphic setting on mangrove tree growth in Micronesia. Biotropica 39 (2), 161–170.
Langmuir, D., 1997. Aqueous Environmental Chemistry. Prentice-Hall, Upper Saddle River, NJ, p. 600.
Lewis, E., 1980. The practical salinity scale 1978 and its antecedents. IEEE J. Ocean. Eng. 5 (1), 3–8.
Loder, T.C., Reichard, R.P., 1981. The dynamics of conservative mixing in estuaries. Estuaries 4 (1), 64–69.
Loveridge, A., Pitt, K.A., Lucas, C.H., Warnken, J., 2021. Extreme changes in salinity drive population dynamics of Catostylus mosaicus medusae in a modified estuary. Mar. Environ. Res. 168, 105306.
Lugo, A.E., Snedaker, S.C., 1974. The ecology of mangroves. Annu. Rev. Ecol. Systemat. 5 (1), 39–64.
Mazda, Y., 2013. The mangrove ecosystem utilizes physical processes. Global Environ. Res. 17, 165–172.

Mazda, Y., Sato, Y., Sawamoto, S., Yokochi, H., Wolanski, E., 1990. Links between physical, chemical and biological processes in Bashita-minato, a mangrove swamp in Japan. Estuar. Coast Shelf Sci. 31 (6), 817–833.
Mazda, Y., Ikeda, Y., 2006. Behavior of the groundwater in a riverine-type mangrove forest. Wetl. Ecol. Manag. 14 (6), 477–488.
Mazda, Y., Wolanski, E., 2009. Hydrodynamics and Modeling of Water Flow in Mangrove Areas. Coastal Wetlands: an Integrated Ecosystem Approach, pp. 231–262.
Mitra, A., 2020a. Mangroves: a nutrient retention box. In: Mangrove Forests in India. Springer, Cham, pp. 87–114.
Mitra, A., 2020b. Mangroves: a reservoir of biodiversity. In: Mangrove Forests in India. Springer, Cham, pp. 241–291.
Ndongo, B., Mbouendeu, S.L., Tirmou, A.A., Njila, R.N., Dalle, J.D.M., 2015. Tendances pluviométriques et impact de la marée sur le drainage en zone d'estuaire: cas du Wouri au Cameroun. Afr. Sci. Rev. Int. Sci. Technol. 11 (2), 173–182.
Nfotabong-Atheull, A., Din, N., Dahdouh-Guebas, F., 2013. Qualitative and quantitative characterization of mangrove vegetation structure and dynamics in a peri-urban setting of Douala (Cameroon): an approach using air-borne imagery. Estuar. Coast 36 (6), 1181–1192.
Olivry, J.C., 1974. Regime hydrologique du fleuve Wouri et estimation des apports recus par l'estuaire et la mangrove du Wouri. Office de la recherche scientifique et technique outre-mer, ORSTOM. Republique unie du Cameroun, p. 60.
Onguene, R., Pemha, E., Lyard, F., Du-Penhoat, Y., Nkoue, G., Duhaut, T., Njeugna, E., Marsaleix, P., Mbiake, R., Jombe, S., Allain, D., 2014. Overview of tide characteristics in Cameroon coastal areas using recent observations. Open J. Mar. Sci. 5 (1), 81.
Peel, M.C., Finlayson, B.L., McMahon, T.A., 2007. Updated world map of the Köppen-Geiger climate classification. Hydrol. Earth Syst. Sci. 11, 1633–1644, 2007.
Ramatlapeng, G.J., Atekwana, E.A., Ali, H.N., Njilah, I.K., Ndondo, G.R.N., 2021. Assessing salinization of coastal groundwater by tidal action: the tropical Wouri Estuary, Douala, Cameroon. J. Hydrol. Reg. Stud. 36, 100842.
Rivera-Monroy, V.H., De Mutsert, K., Twilley, R.R., Castañeda-Moya, E., Romigh, M.M., Davis, S.E., 2007. Patterns of nutrient exchange in a riverine mangrove forest in the Shark River Estuary, Florida, USA. HIDROBIOLOGICA 17 (2), 169–178.
Robson, B.J., Hamilton, D.P., Webster, I.T., Chan, T., 2008. Ten steps applied to development and evaluation of process-based biogeochemical models of estuaries. Environ. Model. Software 23 (4), 369–384.
Simon, L.N., Raffaelli, D., 2012. Assessing ecosystem effects of smallscale cutting of Cameroon mangrove forests. J. Ecol. Nat. Environ. 4 (5), 126–134.
Smith, J., Burford, M.A., Revill, A.T., Haese, R.R., Fortune, J., 2012. Effect of nutrient loading on biogeochemical processes in tropical tidal creeks. Biogeochemistry 108 (1–3), 359–380.
Twilley, R.R., 1985. The exchange of organic carbon in basin mangrove forests in a southwest Florida estuary. Estuar. Coast Shelf Sci. 20 (5), 543–557.
Webb, K.L., 1981. Conceptual models and processes of nutrient cycling in estuaries. In: Estuaries and Nutrients. Humana Press, pp. 25–46.
Willy, S.E., 2016. Analyse de la vulnérabilité du littoral du Wouri: Cartographie des zones à risques d'inondation à Douala. Mémoire d'ingénieur Halieute de l'Institut des sciences halieutiques de l'université de Douala.
Wolanski, E., Mazda, Y., Furukawa, K., Ridd, P., Kitheka, J., Spagnol, S., Stieglitz, T., 2001. Water Circulation in Mangroves, and its Implications for Biodiversity. Oceanographic Processes of Coral Reefs: Physical and Biological Links in the Great Barrier Reef, pp. 53–76.
Wolanski, E., Ridd, P., 1986. Tidal mixing and trapping in mangrove swamps. Estuar. Coast Shelf Sci. 23 (6), 759–771.
Zogning, A., 1993. Les mangroves du Cameroun. Conserv. Utilisation Ration. des For. Mangrove l'Am. Latine Afr. 2, 189–196.